ELSEVIER

Journal of Organometallic Chemistry 572 (1999) 271–281

Journal of Organometallic Chemistry

Mechanistic study of the photoisomerization of $Os_3(CO)_{10}(L)$ in which L (L = 1,4-di-R-1,4-diazabutadiene (R-DAB) or pyridine-2-carbaldehyde *N*-R-imine (R-PyCa)) changes its coordination from σ, σ-N,N′ into σ-N, μ_2-N′, η^2-C=N′

Jos Nijhoff, Maarten J. Bakker, František Hartl, Derk J. Stufkens *

Anorganisch Chemisch Laboratorium, Institute of Molecular Chemistry, Universiteit van Amsterdam, Nieuwe Achtergracht 166, 1018 WV Amsterdam, Netherlands

Received 4 August 1998

Abstract

The triangular clusters $Os_3(CO)_{10}(\alpha$-diimine) photoisomerize to give the imine-bridged clusters $Os_3(CO)_{10}(\sigma$-N, μ_2-N′, η^2-C=N′-α-diimine) if the α-diimine has a reactive imine bond as in the case of R-DAB (1,4-di-R-1,4-diazabutadiene) or R-PyCa (pyridine-2-carbaldehyde N-R-imine). The products are identified by comparing their spectroscopic (IR, UV–vis, ^{1}H-NMR) data with those of compounds reported in the literature. The quantum yield of the photoreaction decreases with an increase of the steric bulk of the α-diimine. Upon irradiation at low temperature the clusters produce unstable species, which transform into the final products on raising the temperature. The R-PyCa clusters produce a single intermediate, the R-DAB clusters three different ones. Some intermediates are assigned by comparing their IR and UV–vis spectra with those of known species. A reaction mechanism is proposed for the photoisomerization, in which visible excitation causes the homolytic cleavage of an Os–Os bond with formation of a biradical. This biradical undergoes an intramolecular radical coupling reaction of the $Os^+(CO)_2(\alpha\text{-diimine}^{\bullet -})$ and $^{\bullet}Os(CO)_4$ radical sites with formation of an imine-bridged species, which is unstable because of a mismatch between the coordination of the two Os atoms. This mismatch is lifted by transfer of a CO ligand from one Os to the other via two CO-bridged (Os–CO–N) intermediates, which are detected at low temperature. This mechanism depicts a route along which the CO ligands of a cluster may move to compensate for an unbalance in metal-coordination.

Keywords: Photisomerization; 1,4-di-R-1,4-Diazabutadiene; Pyridine-2-carbaldehyde; N-R-imine; Os_3 clusters

1. Introduction

Metal–metal bonded complexes such as $M_2(CO)_{10}$ (M = Mn, Re), $Cp_2Fe_2(CO)_4$, and $Cp_2M_2(CO)_6$ (M = Mo, W) undergo metal–metal bond homolysis and release of CO as primary photoprocesses [1–4]. The homolysis reactions lead to the formation of radicals; the CO-loss reactions produce carbonyl-bridged species [5,6]. A detailed photochemical study has shown that similar homolysis reactions not only occur for the corresponding α-diimine (bpy, etc.) substituted complexes $M_2(CO)_8(\alpha$-diimine) (M = Mn, Re) [7,8], but also for a great variety of other metal–metal bonded complexes such as $L_nM'M(CO)_3(\alpha$-diimine) (L_nM' = $(CO)_4Co$, $Cp(CO)_2Fe$, Ph_3Sn; M = Mn, Re) [7–22], $L_nM'Ru(Me)(CO)_2(\alpha$-diimine) ($L_nM' = (CO)_5Mn$, $(CO)_5Re$, $(CO)_4Co$, $SnPh_3$, $PbPh_3$) [23,24], and $Ru(SnPh_3)_2(CO)_2(\alpha$-diimine) [24,25].

The fate of the metal radicals was studied in most detail for the complexes $(CO)_5MnMn(CO)_3(\alpha$-diimine). As long as the solvent is non-coordinating and nonvis-

* Corresponding author. Tel.: +31-20-525-6451; fax: +31-20-525-6456; e-mail: stufkens@anorg.chem.uva.nl.

0022-328X/99/$ - see front matter
PII: S0022-328X(98)00955-3

cous, the $^{\bullet}Mn(CO)_5$ and $Mn(CO)_3(\alpha\text{-diimine})^{\bullet}$ radicals diffuse from the solvent cage and dimerize to give $Mn_2(CO)_{10}$ and $Mn_2(CO)_6(\alpha\text{-diimine})_2$, respectively [7]. In coordinating solvents or in the presence of N- or P-donor ligands (L) the complexes photodisproportionate into the ions $Mn(CO)_5^-$ and $Mn^+(CO)_3(L)(\alpha\text{-diimine})$ [14,26]. Apart from these dimerization and disproportionation reactions, the radicals may yet undergo another reaction in a viscous solvent (e.g. paraffin), in which they cannot diffuse from the solvent cage. In such a medium a radical coupling reaction occurs with release of CO and formation of an α-diimine-bridged photoproduct, provided the α-diimine contains a reactive imine bond as in the case of R-DAB (1,4-di-R-1,4-diazabutadiene) and R-PyCa (pyridine-2-carbaldehyde-N-R-imine) (see Fig. 1) [7,23]. Our investigations have clearly shown that these dimers, ion pairs and ligand-bridged complexes are all secondary products of the radicals.

Recently, we have extended these investigations to triangular clusters of the type $Os_3(CO)_{10}(\alpha\text{-diimine})$ [27,28], which indeed show a similar homolytic cleavage of a metal–metal bond on irradiation into their visible absorption band. However, as their photofragments remain bonded to each other by the bridging $Os(CO)_4$ group, quite different photoproducts are obtained for these clusters. Thus, instead of two separate radicals, these clusters produce biradicals, which were identified with nanosecond time-resolved absorption spectroscopy and with EPR spectroscopy as their adducts with nitrosodurene [28]. In non- and weakly coordinating solvents (toluene, THF) these biradicals normally regenerate the parent cluster within 10–1000 ns, depending on the solvent and the α-diimine. In the presence of an excess of acetonitrile or pyridine (S), the biradicals transform into the zwitterions $(CO)_4Os^- - Os(CO)_4 - Os^+(S)(CO)_2(\alpha\text{-diimine})$. The latter zwitterions are formed as primary photoproducts in neat acetonitrile and pyridine. Their lifetime depends mainly on the coordinating ability of S, varying from seconds in the case of acetonitrile to minutes for pyridine at room temperature (r.t.). Apparently, the electron transfer reaction by which the $^{\bullet}Mn(CO)_5$ and $Mn(CO)_3(\alpha\text{-diimine})^{\bullet}$ radicals transform into the ions $Mn(CO)_5^-$ and $Mn(CO)_3(S)(\alpha\text{-diimine})^+$, respectively, has its counterpart in the transformation of the biradicals $^{\bullet}(CO)_4Os - Os(CO)_4 - Os(CO)_2(\alpha\text{-diimine})^{\bullet}$ into the zwitterions $(CO)_4Os^- - Os(CO)_4 - Os^+(S)(CO)_2(\alpha\text{-diimine})$. Importantly, the occurrence of the latter reaction not only depends on the coordinating ability and electron donating character of S, but also on the π-accepting properties of the α-diimine [28].

The mechanism proposed for these reactions is schematically depicted in Scheme 1 [28]. The visible absorption band of the clusters arises from metal-to-ligand charge transfer (MLCT) transitions from close-lying $d_\pi(Os)$ and $\sigma(Os_3)$ orbitals to the lowest π^* orbital of the α-diimine ligand [29]. Irradiation into these transitions eventually leads to the occupation of a reactive $^3\sigma(Os_3)\pi^*(\alpha\text{-diimine})$ state, from which the biradicals are formed by homolysis of an Os–Os bond. As mentioned above the biradicals normally regenerate the parent cluster, either directly, or via the zwitterion [28]. For the clusters containing an R-DAB or R-PyCa ligand with a reactive imine bond, regeneration of the parent cluster is, however, not the only reaction. In order to find out if this is due to the fact that part of the biradicals undergo an intramolecular coupling reaction, comparable to that between the Mn-radicals in viscous media [7], this sidereaction was studied in more detail for several $Os_3(CO)_{10}(\alpha\text{-diimine})$ (L = R-DAB or R-PyCa) clusters. In this article we report the results of this investigation for the clusters depicted in Fig. 1

2. Experimental

2.1. Materials and preparations

2-Pyridinecarboxaldehyde (Acros) and *N*,*N*-dimethyl-ethylenediamine (Aldrich) were used as purchased. Solvents of analytical (acetonitrile, *n*-hexane and THF) or spectroscopic grade (toluene, dichloromethane, 2-chlorobutane) quality were dried over sodium wire (THF, toluene, *n*-hexane) or CaH_2 (acetonitrile, dichloromethane, 2-chlorobutane) and freshly distilled under nitrogen. Pyridine, acetonitrile and butyronitrile were stored on molecular sieves.

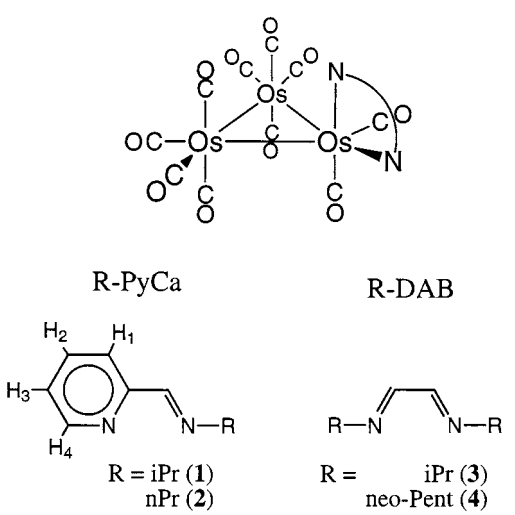

Fig. 1. Schematic structure of the clusters $Os_3(CO)_{10}(\alpha\text{-diimine})$ and of the α-diimine ligands used.

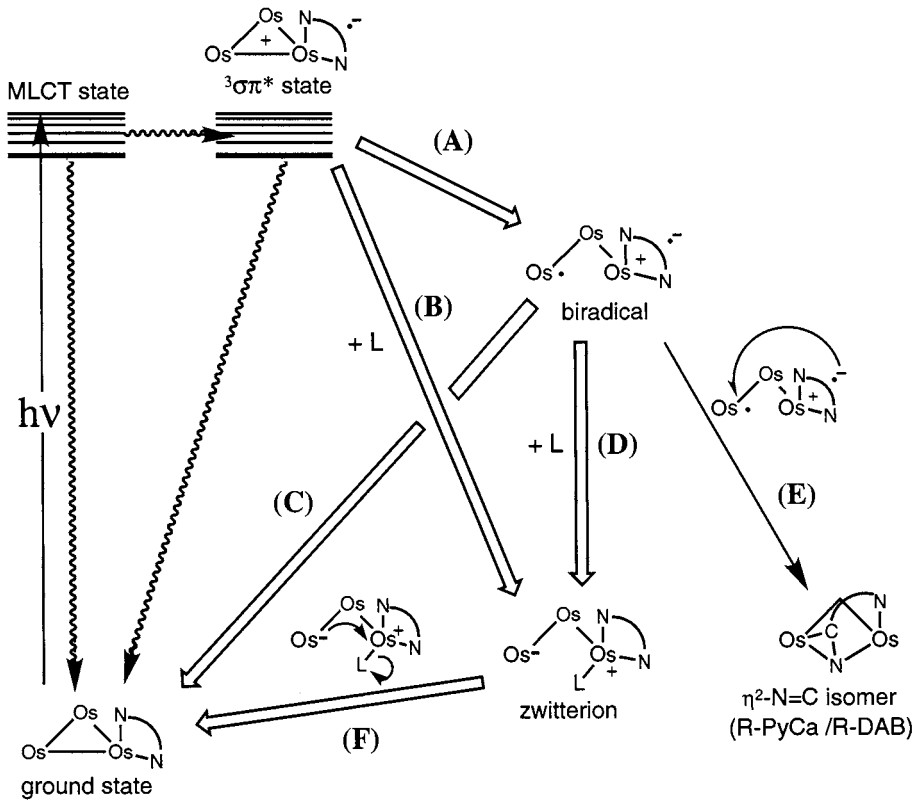

Scheme 1. General scheme for the photoreactions of the clusters $Os_3(CO)_{10}(\alpha$-diimine). The separate reaction steps (**A**)–(**F**) depend on the solvent used: (i) (**A**) + (**C**) and (**A**) + (**E**) in toluene, 2-chlorobutane and THF. (ii) (**B**) + (**F**) and/or (**A**) + (**D**) + (**F**) in acetonitrile and pyridine (iii) (**A**) + (**D**) + (**F**) in THF + 0.5 M CH_3CN.

The clusters 1–**4** were prepared following published procedures [28,30,31].

2.2. $Os_3(CO)_{10}(Me_2N–(CH_2)_2–AcPy)$ (**5**)

The complex $Os_3(CO)_{10}(Me_2N–(CH_2)_2–AcPy)$ (**5**) was prepared analogously [28], using the appropriate α-diimine ligand. IR (ν(CO) in cm^{-1}; in 2-chlorobutane): 2085 m, 2036 s, 2007 s, 1993 s, 1978 s, 1962 m, 1958 sh, 1907 w. ^{1}H-NMR (δ in ppm; in $CDCl_3$): 9.52 (d, 1H, H4), 7.99 (d, 1H, H1), 7.85 (dt, 1H, H2), 7.21 (dt, 1H, H3), 4.57 (m, 1H, =N–C$\underline{H}_2$), 4.38 (m, 1H, =N–C$\underline{H}_2$), 2.82 (m, 2H, $\underline{CH}_2NMe_2$), 2.62 (s, 3H, N=C–$\underline{CH}_3$), 2.32 (s, 6H, N$\underline{Me}_2$). UV–vis (λ_{max} in nm (ε_{max} in M^{-1} cm^{-1}); in THF): 549 (5300). Mass (FAB^+): $(m/z)^+$ 1043 ([M^+] 1042.00 calc.).

2.3. Reaction of $Os_3(CO)_{10}(CH_3CN)_2$ with ^{i}Pr-DAB (*N,N′-diisopropyl-1,4-diaza butadiene*)

A total of 870 mg of $Os_3(CO)_{10}(CH_3CN)_2$ and one equivalent of ^{i}Pr-DAB were dissolved in 200 ml of THF and allowed to react under rigorous exclusion of light as described in Ref. [28]. The yield of **3** was 359 mg (36%) and of **3a** (see Section 3) 30 mg (3%) after column chromatography and recrystallisation from *n*-hexane.

2.4. Spectroscopic measurements

UV–vis absorption spectra were recorded with a Varian Cary 4E spectrophotometer and FTIR spectra with a Bio-Rad FTS-7 spectrometer (16 scans, 2 cm^{-1} resolution). Real-time (RT, 'rapid scan') FTIR spectra were measured with a Bio-Rad FTS-60A spectrometer [32]. Low temperature IR and UV–vis measurements were performed using an Oxford Instruments DN 1704/54 liquid nitrogen cryostat equipped with CaF_2 and quartz windows. ^{1}H-NMR spectra were recorded with a Bruker AMX 300 spectrometer.

2.5. Photochemistry

A Spectra Physics 2025 argon-ion laser was used as the light source for the photochemical experiments, unless stated otherwise. The light-sensitive samples (10^{-3}–10^{-4} M) were prepared in a carefully blinded room, illuminated with red light. In order to measure their ^{1}H-NMR spectra, photoproducts **1a**–**4a** (see Section 3) were prepared in a rather high concentration by irradiation of 2×10^{-3} M solutions of **1**–**4** in dichloromethane in a home-made, large-volume, thin-layer cell [33]. The photochemical conversion was monitored in situ by FTIR spectroscopy. When ca. 80% of

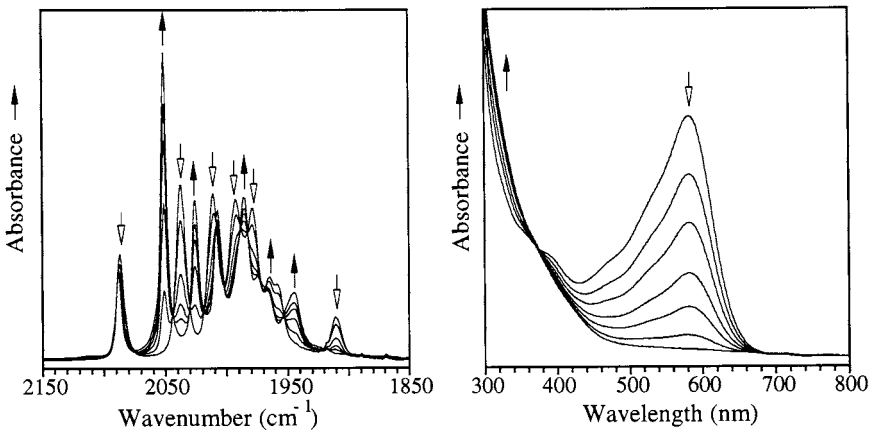

Fig. 2. IR (left) and UV–vis (right) spectral changes accompanying the formation of photoproduct **1a** by irradiation of **1** in toluene at 298 K.

the parent cluster had reacted, the solution was transferred to a Schlenk tube. The solvent was evaporated and the residue was redissolved in $CDCl_3$ and subsequently transferred to an NMR tube.

Quantum yields of the disappearance of the parent clusters were determined by recording the decrease of the intensity of their visible absorption band as a function of the number of photons absorbed, following an automated procedure. During the measurements the sample was kept in a thermostated 1 cm cuvette within the UV–vis spectrophotometer, and irradiated with one of the argon-ion laser lines via an optical fibre. The solution was well stirred during the irradiation intervals, and the conversion per interval was kept below 5%. These intervals were realized using a computer-controlled mechanical shutter. Light intensities were measured with a Coherent 212 power meter which was calibrated with an Aberchrome 540 solution according to literature procedures [36,37]. In the computational routine [34] corrections were made for changes in the partial absorption of the photoactive species caused by both its depletion and by the inner filter effect of the photoproduct(s) formed.

3. Results and discussion

The photoreactions of the clusters $Os_3(CO)_{10}(\alpha$-diimine) (**1**–**4**) were studied at r.t. by irradiation into the visible absorption band with the 514.5 nm line of an argon-ion laser, unless stated otherwise. Several reactions were investigated in more detail at lower temperatures in order to stabilize and identify reactive intermediates. The photoreactions were studied for solutions of the clusters in weakly or noncoordinating solvents such as THF, CH_2Cl_2, 2-chlorobutane, toluene or *n*-hexane.

3.1. Photolysis at room temperature

3.1.1. Formation and characterization of the final photoproducts

Irradiation of the clusters $Os_3(CO)_{10}$(R-PyCa) (R = ^{i}Pr, **1**; R = ^{n}Pr, **2**) gave rise to the formation of stable photoproducts, to be denoted as **1a** and **2a**, respectively. The reactions were followed with IR (CO-stretching region) and UV–vis spectroscopy; the spectral changes accompanying the conversion of **1** into **1a** are presented in Fig. 2. The IR (ν(CO)) spectral patterns of **1a** and **2a** are completely different from those of the parent clusters **1** and **2** (see Fig. 2 and Table 1). They are dominated by a strong and sharp ν(CO) band at ca. 2050 cm^{-1}. During the reaction of cluster **2**, additional ν(CO) bands appear at 2098 (w), 2075 (w), 2060 (sh), 2019 (s) and 1937 (sh) cm^{-1} (in toluene), pointing to the formation of a side product in low concentration ($< 10\%$). Due to its low yield and thermal instability, this product was not further investigated.

The photoreaction causes the disappearance of the visible MLCT band (at ca. 580 nm in toluene); at the same time the absorption between 300 and 400 nm increases slightly, giving rise to a shoulder extending to 440 nm.

In order to measure its ^{1}H-NMR spectrum, a rather concentrated solution of **1a** was prepared by irradiation of **1** (see Section 2). In the ^{1}H-NMR spectrum the resonance of the imine proton of **1** had shifted from 8.86 to 4.38 ppm on formation of **1a** and the isopropyl group had become asymmetric. This is evident from the observation that the signals of its methyl groups, nearly coinciding at 1.57 and 1.54 ppm for cluster **1**, are found as two separate doublets for **1a** at 1.34 and 1.06 ppm, respectively. In addition, the signal of the $-C\underline{H}Me_2$ proton had shifted from 4.77 to 1.85 ppm. Similar shifts are observed on going from **2** to **2a**. As mentioned above, **2a** is not the only product of **2**, and additional

Table 1
NMR data of the photoproducts **1a**–**4a** in $CDCl_3$[a]

1a	8.49 (d, 1H, H4), 7.58 (m, 2H, H1+H2), 6.98 (m, 1H, H3), 4.38 (s, 1H, N=C–H), 1.85 (m, 1H, C<u>H</u>Me$_2$), 1.34 (d, 3H, CH<u>Me$_2$</u>), 1.06 (d, 3H, CH<u>Me$_2$</u>)
2a	8.52 (d, 1H, H4), 7.56 (m, 2H, H1+H2), 6.99 (dt, 1H, H3), 4.45 (s, 1H, N=C–H), 3.93 (dt, 1H, =N–C<u>H$_2$</u>), 3.10 (dt, 1H, =N–C<u>H$_2$</u>), 2.29 (m, 2H, <u>CH$_2$</u>CH$_3$), 1.03 (t, 3H, CH$_2$<u>CH$_3$</u>)
3a	8.47 (s, 1H, N=C–H), 3.95 (m, 1H, C<u>H</u>Me$_2$), 3.64 (d, 1H, N=C–H), 1.77 (m, 1H, C<u>H</u>Me$_2$), 1.48 (d, 3H, CHMe$_2$), 1.46 (d, 3H, CHMe$_2$), 1.37 (d, 3H, CH<u>Me$_2$</u>), 1.04 (d, 3H, CH<u>Me$_2$</u>)
4a	8.28 (s, 1H, N=C–H), 3.91 (d, 1H, C<u>H$_2$</u>–^{t}Bu), 3.78 (s, 1H, C<u>H$_2$</u>–^{t}Bu), 3.77 (s, 1H,C<u>H$_2$</u>–^{t}Bu), 3.68 (d, 1H, N=C–H), 2.38 (d, 1H, C<u>H$_2$</u>–^{t}Bu), 1.22 (s, 9H, CH$_2$–^{t}<u>Bu</u>), 1.12 (s, 9H, CH$_2$–^{t}<u>Bu</u>)

[a] For numbering scheme see Fig. 1.

resonances are observed at 7.72 (dt), 6.89 (t), 5.35 (t), 3.76 (m), and 2.00 (m) ppm.

The clusters $Os_3(CO)_{10}$(R-DAB) (R = ^{i}Pr, **3**; R = neoPent, **4**) behave similarly on irradiation in weakly- or noncoordinating solvents. Their photoproducts **3a** and **4a** have almost the same ν(CO) stretching frequencies as **1a** (see Table 2). Moreover, just as for clusters **1** and **2**, the visible absorption bands of **3** and **4** disappear on irradiation while a shoulder remains at ca. 350 nm. In one respect, however, the photochemical behaviour of **3** and **4** differs from that of **1** and **2**. Irradiation of **3** or **4** dissolved in a nitrile solvent affords again **3a** or **4a**, respectively, whereas **1** and **2** produce instead zwitterions of the type $(CO)_4Os^- – Os^+(S)(CO)_2$($\alpha$-diimine), denoted as **1b** and **2b**, respectively. The formation of these zwitterions as well as their properties have been discussed in detail in a previous article [28]. The ^{1}H-NMR spectra of **3a** and **4a** show features which are very similar to those of **1a** and **2a**. In contrast to their parent clusters **3** and **4**, the imine protons and the R-groups of **3a** and **4a** are magnetically inequivalent. Two resonances are observed for the imine protons: one has shifted to a much lower ppm value (**3a**: 3.64 ppm; **4a**: 3.68 ppm) while the other signal is still observed above 8 ppm.

The IR and ^{1}H-NMR data of **1a**–**4a** closely correspond to those reported by Zoet et al. [30,31] for the imine-bridged cluster $Os_3(CO)_{10}$(σ-N, μ_2-N′, η^2-C=N′-α-dimine). The authors determined the crystal structure of the cyclopropyl-DAB product, which is schematically depicted in Fig. 3 (left). One of the Os–Os bonds is broken, but the two metal atoms are still connected by an imine group, which is σ bonded to one osmium atom and η^2-bonded to the other. To compensate for this η^2 coordination, a CO ligand has been transferred from the η^2-bond forming osmium atom to that of the $Os(CO)_2$(α-dimine) moiety, i.e. from left to right in Fig. 3. The formation of this imine η^2-bond explains the disappearance of the MLCT band during the conversion of **1**–**4** into **1a**–**4a**. Due to the η^2-bond formation, the π-conjugation within the α-diimine is lifted causing the disappearance of the transitions to a low-lying π*-orbital.

Zoet et al. prepared and isolated products **1a**, **3a** and **4a** from the thermal reaction of $Os_3(CO)_{10}(CH_3CN)_2$ with the appropriate R-PyCa or R-DAB ligand. In most cases the imine-bridged species was only a minor product, the major product being cluster **1**, **3** or **4**. Only in a few cases, depending on the medium and the bulkiness of the R-group, the imine-bridged species, which is in fact an isomer of the σ-N,σ-N′ bonded α-diimine cluster, became the major product. For instance, the σ-N, μ_2-N′, η^2-C=N′-bonded isomer was the only product formed in the thermal reaction of $Os_3(CO)_{10}(CH_3CN)_2$ with cyclopropyl-DAB [31].

In order to find out if the latter reactions had been (partly) induced by light, $Os_3(CO)_{10}(CH_3CN)_2$ was allowed to react with ^{i}Pr-DAB in complete darkness. Although the yield of **3a** was lower and that of **3** higher than those reported by Zoet et al. a significant amount of **3a** was still obtained in the absence of light. This proves that **1a**–**4a** can be prepared both thermally and photochemically, most probably via different pathways. Evidence for a different mechanism was provided by the observation that the solvent has an opposite effect on both reactions. For, the yield of the thermal reaction was higher in toluene, whereas that of the photochemical reaction was higher in THF.

In a previous article we have shown that irradiation of **1**–**4** in toluene gives rise to the formation of biradicals since their adducts with the spin trap nitrosodurene could be detected by EPR spectroscopy [28]. The same biradicals are, apparently, intermediates of the photo-transformation of **1**–**4** into **1a**–**4a**. For, irradiation of **1** or **3** in toluene in the presence of an excess of nitrosodurene or ^{t}BuNO did not produce **1a** or **3a**, but other, thermally unstable, species, which decomposed on standing. We therefore conclude that **1a**–**4a** are formed via a radical pathway.

Table 2
IR data (ν(CO) in cm^{-1}) of the clusters **1**–**4**, of the photoproducts **1a**–**4a** recorded in toluene at room temperature, and of the low temperature photoproducts **1′**–**4″** recorded in 2-chlorobutane and **3b**, **3*(S)** and **4″** in butyronitrile

1	2087 m	2037 s	2011 s	1993 s	1979 s	1965 m	1959 m	1910 w
1′[a]	2115 m	2061 vs	2043 w	2024 vs	1994 sh	1981 m	1975 sh	1906 w
1a	2088 m	2051 vs	2026 m	2007 m	1986 m	1975 m	1967 w	1945 w
2	2088 m	2038 s	2011 s	1993 s	1979 s	1966 m	1959 m	1911 w
2′[a]	2115 m	2060 vs	2043 w	2024 vs	1990 sh	1981 s	1975 sh	1908 w
2a	2089 m	2053 vs	2027 m	2007 m	1988 s	1977 sh	1968 sh	1951 sh
3	2096 m	2048 s	2019 s	2003 s	1992 s	1976 m	1961 w	1914 w
3″[b]	2092 w	2052 vs	2018 s	1989 m	1964 sh	1957 w	1935 vw	
3a	2089 m	2051 vs	2027 s	2007 s	1981 m	1974 sh	1967 m	1947 m
3b[c]	2078 w	2022 w	2001 s	1997 sh	1975 vs	1942 w	1902 w	1877 m
3*(S)[d]	2085 m	2037 s	2004 vs	1990 s	1970 m	1951 m	1932 w	1692 vw
4	2101 m	2054 s	2023 s	2013 s	1995 s	1979 m	1961 m	1913 w
4″[b]	2110 m	2061 s	2029 s	2010 m	1999 s	1984 m	1925 m	1721 w
4″[c]	2113 m	2058 s	2010 s	1995 s	1979 m	1947 w	1916 m	1708 w
4b	2090 m	2053 vs	2030 s	2007 s	1984 s	1975 sh	1969 m	1951 w

[a] At 183 K.
[b] At 223 K in 2-chlorobutane.
[c] At 223 K in butyronitrile.
[d] At 243 K in butyronitrile.

3.2. Quantum yield measurements

In order to obtain further information on the reaction mechanism and, in particular, on the influence of the imine substituents on the efficiency of the formation of **1a**–**4a**, the quantum yields for the disappearance of the parent clusters **1**–**4** were determined in toluene, THF and acetonitrile. The resulting data, collected in Table 3, show that the quantum yield varies rather strongly from one cluster to another, and generally increases on going to a more strongly coordinating solvent. For clusters **1**, **2** and **4** in THF the quantum yield was also determined at three different wavelengths of irradiation. No significant variation in quantum yield was observed; only in the case of cluster **2** the quantum yield slightly increased on excitation at shorter wavelength. The consequences of these results for the reaction mechanism will be discussed in a later section.

3.3. Photolysis at low temperatures

For the study of the photochemical reactions at lower temperatures, 2-chlorobutane was preferred as an apolar solvent since it has only very weak absorptions in the 2200–1600 cm^{-1} IR region. The first important observation was that all photoproducts, obtained by irradiation of the clusters at $T < 200$ K, transformed into the ligand-bridged isomers **1a**–**4a** and partly into the parent clusters on raising the temperature. This means that these low-temperature products are reactive intermediates of the photoisomerization, which therefore give valuable information about the mechanism of this reaction. Moreover, different intermediates were observed for clusters **1**–**4**, which provided an even more detailed picture of the reaction path.

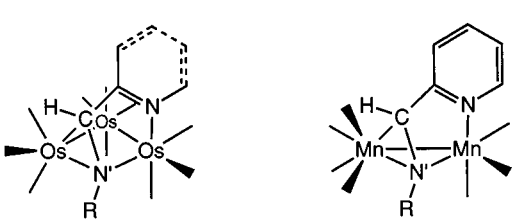

Fig. 3. Schematic structure of the photoproducts $Os_3(CO)_{10}(\sigma$-N, μ_2-N′, η^2-C=N′-L) (L = α-diimine = R-DAB or R-PyCa) (left) and $(CO)_3Mn(\sigma$-N, μ_2-N′, η^2-C=N′-R-PyCa)$Mn(CO)_3$ (right).

Irradiation of **1** or **2** in 2-chlorobutane at 183 K affords a new species, to be denoted as **1′** or **2′**, respectively. The wavenumbers of the three highest-frequency ν(CO) bands of **1′** and **2′** (Table 2) are 16–28 cm^{-1} larger than those of **1** and **2**. The weak lowest-frequency band has hardly changed, while the remaining bands have become much weaker. Apart from these changes, the overall IR patterns of **1′** and **2′** are similar to those of **1** and **2**, respectively (Fig. 4a). On the other hand, the visible MLCT band disappears on going from **1** to **1′** and from **2** to **2′**, just as upon irradiation at r.t. When the temperature of the 2-chlorobutane solution is raised to 203 K, a small amount of **1a** and **2a** is formed as evidenced by the appearance of a weak ν(CO) band at 2051 cm^{-1}. The main part of **1′** and **2′**, however, regenerates the parent cluster. When the reaction is instead performed at 213 K, the intermediate **1′** reacts further to give **1a** as the major (> 80%) photoproduct. Species **1′** is also formed on irradiation of a solution of **1** in CH_2Cl_2 at 213 K. By raising the temperature to 233 K, **1′** is then transformed into **1a** and into a small amount of **1**. Because of the low efficiency of their formation (vide infra) and their thermal instability,

Table 3
Quantum yields $\Phi\ 10^2$ at 298 K[a] for the disappearence of **1**–**4** on 514.5 nm irradiation in toluene and acetonitrile and at different irradiation wavelengths λ_{irr} (in nm) in THF

Solvent	Toluene	THF			Acetonitrile
λ_{irr}	514.5	457.9	488.0	514.5	514.5
1	0.197	0.295	0.319	0.299	[b]
2	1.60	3.67	3.48	3.27	[b]
3	0.166	[c]	[c]	0.813	5.24
4	1.75	1.66	1.66	1.64	3.38

[a] $T \pm 0.1$ K; estimated relative error ca. 3%
[b] A different photoreaction (zwitterion formation) was observed.
[c] Wavelength dependence of Φ was not determined.

intermediates **1′** and **2′** could not be further analysed with ^{1}H-NMR spectroscopy.

A different species is obtained on irradiation of $Os_3(CO)_{10}(^i$Pr-DAB) (**3**) in 2-chlorobutane at 223 K, as well as in CH_2Cl_2 and THF at $T < 253$ K. The IR spectrum of this intermediate, to be denoted as **3‴**, is different from that of **1′** and **2′**, but very similar to that of photoproduct **3a**, obtained by irradiation of **3** at r.t. (Fig. 4b). As for **3a**, a strong ν(CO) band is observed in the spectrum of **3‴** at 2050 cm^{-1}. However, **3‴** has only one strong band at 2018 cm^{-1} instead of two weaker ones observed for **3a** at 2027 and 2007 cm^{-1}, respectively. Raising the temperature to 273 K causes **3‴** to react further to give the imine-bridged isomer **3a**. Similar results were obtained for the clusters dissolved in CH_2Cl_2 or THF.

Finally, still another intermediate was obtained in the case of $Os_3(CO)_{10}$(neoPent-DAB) (**4**). Irradiation of this cluster at 223 K in 2-chlorobutane causes the formation of a product, to be denoted as **4″**. This intermediate has a ν(CO) band pattern (see Fig. 4c) which is quite different from that of the intermediates **1′**, **2′**, **3‴**, and of the photoproduct **4a**. It has no sharp and intense ν(CO) band at 2050 cm^{-1} as **4a**, but only a moderately strong band at 2060 cm^{-1}. In addition, the IR spectrum of **4″** shows strong bands at 2029, 2010 and 1999 cm^{-1} and, importantly, a weak absorption at 1721 cm^{-1}, i.e. in the frequency region of the bridging carbonyls. Raising the temperature to 243 K causes again the thermal transformation of intermediate **4″** into the isomer **4a**.

According to the r.t. experiments (vide supra), the photoreaction of the R-PyCa clusters **1** and **2** in acetonitrile differs from that of the R-DAB clusters **3** and **4** in this solvent. Clusters **1** and **2** transform into zwitterions, which do not react further to give **1a** and **2a**, but regenerate the parent clusters. In contrast to this, irradiation of **3** and **4**, which have a strongly delocalized Os–(R-DAB) interaction [28,29], produces the isomers **3a** and **4a**, respectively. In order to discover if **3** and **4** still produce zwitterions at low temperatures, the photochemistry of these clusters was studied in butyronitrile at 223 K. Irradiation of **3** then produces indeed the zwitterion **3b**. The charge-transfer band in the visible region does not disappear and its maximum merely shifts by ca. 5 nm to a longer wavelength with respect to that of the parent cluster. On further irradiation, or on raising the temperature to 243 K, **3b** reacts further to give a new species, to be denoted hereinafter as **3*(S)**. The CO-stretching frequencies of **3*(S)** are clearly different from those of **3‴**, obtained by irradiation of **3** in 2-chlorobutane (vide supra) (compare spectra in Fig. 4c). The two highest-frequency ν(CO) bands of **3‴** are still present in the spectrum of **3*(S)**, but they have sharpened considerably. From the bands in the middle of the carbonyl-stretching region, the band at 2004 cm^{-1} is strong, whereas the others are much weaker. Most remarkable, however, is the presence of a weak ν(CO) band at 1692 cm^{-1}. At 243 K the intermediate **3*(S)** starts to convert slowly into **3a**, but at 298 K it still has a lifetime of a few seconds.

Contrary to **3**, cluster **4** does not produce the zwitterion **4b** on irradiation in butyronitrile at temperatures as low as 173 K. At 223 K this cluster shows the same photoreaction in butyronitrile as in 2-chlorobutane. Again species **4″** (see Table 2) is formed, which is thermally stable at this temperature. Its bridging carbonyl vibration shifts from 1721 in 2-chlorobutane to 1708 cm^{-1} in butyronitrile.

3.4. The structures of the intermediates

The above results show that there is a close similarity between the photochemistry of the clusters under study and that of the binuclear metal–metal bonded complexes $(CO)_5MnMn(CO)_3(\alpha$-diimine). The clusters produce biradicals, the binuclear complexes photodecompose into radicals. Both the radicals and biradicals undergo a coupling reaction producing an α-diimine-bridged photoproduct in the case of the R-DAB and R-PyCa complexes.

Although both reactions proceed via a radical mechanism, their conditions and products are not the same. Thus, in the case of the binuclear complexes the coupling reaction is only efficient in viscous media since the

radicals must stay together in the solvent cage. In the case of the Os-clusters the viscosity of the solvent is not of importance anymore since the two radical sites are connected in the biradical species. Moreover, the products of the binuclear complexes and the triangular clusters are also not the same as can be seen from Fig. 3. Irradiation of the Mn-complexes produces $^{\bullet}Mn(CO)_5$ and $Mn(CO)_3(\alpha\text{-diimine})^{\bullet}$ radicals. During the coupling reaction of these radicals in viscous media, η^2 coordination of the α-diimine ligand is compensated by CO loss from the $Mn(CO)_5$ fragment. In the case of the Os-clusters the $^{\bullet}Os(CO)_4$ radical fragment, formed by homolysis of an Os–Os bond, loses CO also. However, in contrast to the Mn–Mn bonded complexes, this CO ligand is not released but transferred to the $Os(CO)_2(\alpha$-diimine) fragment and the Os–Os bond remains broken.

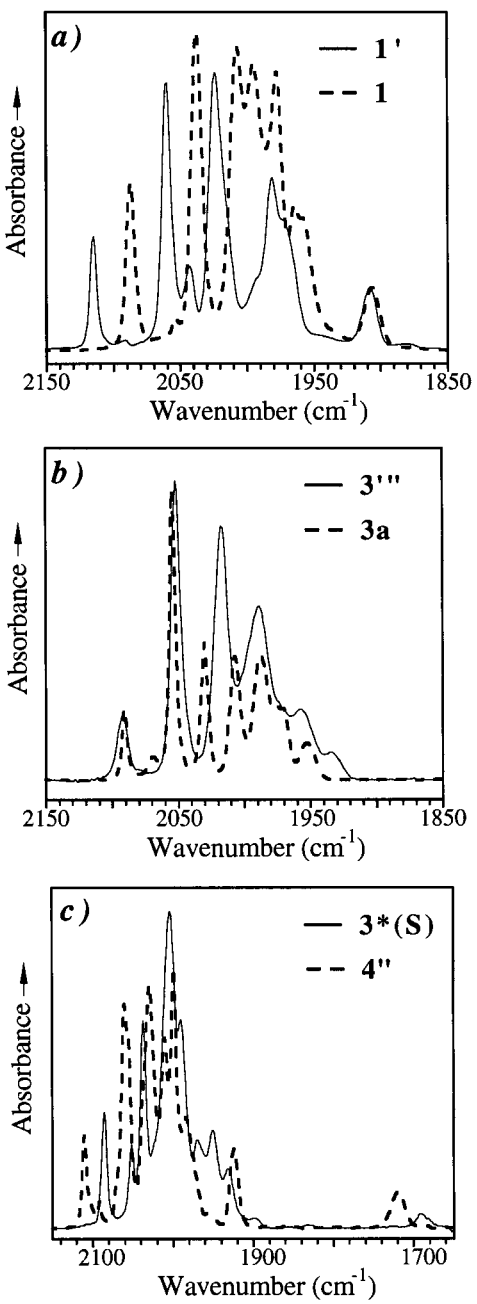

Fig. 4. FTIR spectra (CO stretching region) of (a) **1′** (solid line, in 2-chlorobutane at 183 K) and **1** (dashed line; in toluene at 295 K) (b) **3‴** (solid line, at 223 K) and **3a** (dashed line, at 273 K) in 2-chlorobutane (c) **3*(S)** (solid line) at 223 K in butyronitrile and **4″** (dashed line, at 223 K) in 2-chlorobutane.

The reaction involves a radical coupling reaction between the $^{\bullet}Os(CO)_4$ and $Os(CO)_2(\alpha$-diimine)$^{\bullet}$ radical fragments of the biradical. Steric effects of the imine group are expected to influence the efficiency of this reaction. This is indeed the case, as can be seen from the quantum yield data of Table 3. On going from the ^{i}Pr-PyCa cluster **1** to cluster **2**, containing the less bulky ligand ^{n}Pr-PyCa, the quantum yield increases by a factor of ten. A similar effect is observed for clusters **3** and **4**. In agreement with this, the photoisomerization does not occur at all when the hydrogen of the imine carbon atom is replaced by a methyl group, as in the clusters $Os_3(CO)_{10}$(R-AcPy) (R = ^{i}Pr, ^{n}Pr; AcPy = 2-acetylpyridine *N*-alkylimine) [28,29].

It has been shown in the previous section that all the unstable species **1′**, **2′**, **3‴**, **4″** and **3*(S)** transform into **1a**–**4a**, respectively, and are, therefore, intermediates of the photoisomerization reaction. Although this cannot be proven, we assume that they are intermediates of the same reaction sequence, stabilized at different stages of the process of metal–metal bond cleavage, η^2-bond formation and CO migration. They have in common that they do not possess a strong absorption band in the visible region as the parent clusters and zwitterions do. According to their IR spectra, **1′** (**2′**), **3‴**, **4″** and **3*(S)** have different structures, which could not further be established with ^{1}H-NMR spectroscopy because of the low efficiences of the photoreactions and the photolability of the intermediates. In some cases these IR spectra are, however, revealing since they correspond very closely to those of clusters for which the crystal structure has already been determined by X-ray diffraction.

Contrary to the R-DAB clusters **3** and **4**, the R-PyCa clusters **1** and **2** show the formation of only one type of intermediate, **1′** and **2′**, respectively, and their photoisomerization reaction only proceeds in weakly- or non-coordinating solvents. These reactions will therefore be discussed first, the more complicated reaction mechanism of **3** and **4** will be treated thereafter. The overall mechanism is summarized in Scheme 2.

Intermediates **1′** and **2′**, observed after irradiation of **1** and **2**, respectively in 2-chlorobutane at 183 K and in CH_2Cl_2 at 213 K, have similar structures since their ν(CO) frequencies are very much alike. Hereinafter they will therefore be referred to as **1′/2′**. Their ν(CO) bands resemble those of **1** and **2**, but they are shifted somewhat to higher frequencies. This means that the π-back-

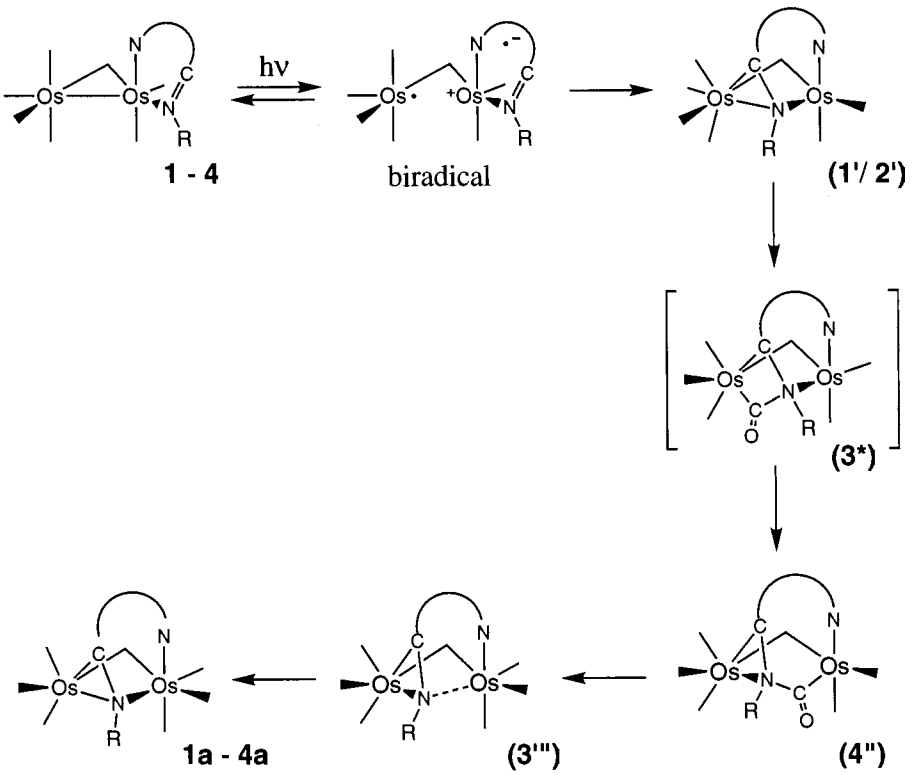

Scheme 2. Proposed scheme for the photoisomerization of the clusters $Os_3(CO)_{10}(\alpha$-diimine) in a weakly- or non-coordinating solvent. The bridging $Os(CO)_4$ groups have been omitted for clarity. Intermediate **3*** was not detected in such solvents but it could be stabilized as **3*(S)** in butyronitrile (see text and Fig. 5).

bonding to the carbonyls has decreased, most probably due to increased π-backbonding to the bridging R-PyCa ligand. This explanation is in agreement with the disappearance of the MLCT band on going from **1/2** to **1′/2′**. It is therefore proposed that homolysis of the Os–Os bond between the $Os(CO)_4$ and $Os(CO)_2$(R-PyCa) moieties is followed by an intramolecular reaction between the $Os(CO)_2$(R-PyCa)$^{\bullet}$ and $^{\bullet}Os(CO)_4$ radical sites of the biradical, resulting in η^2-coordination of the imine group to the other Os atom. In view of the IR spectra, this action has occurred without large structural changes of the Os-carbonyl moieties. The structure proposed for **1′/2′**(see Fig. 5) is therefore not very different from that of the parent cluster, although there is now a mismatch between the coordination spheres of the two osmium atoms. Because of this, intermediates **1′** and **2′** are thermally unstable and transform back into their parent clusters and into products **1a** and **2a**, respectively, in which a carbonyl ligand has moved from one centre to the other to compensate for the mismatch.

The reaction mechanism of the R-DAB clusters **3** and **4** is more complicated, since the type of intermediate formed depends both on the substituent R and on the solvent. For instance, the ^{i}Pr-DAB cluster **3** produces the zwitterion **3b** and the intermediate **3*(S)** in the coordinating solvent butyronitrile, but **3‴** in a non-coordinating solvent, both at low temperature. Cluster **4**, containing the less bulky neoPent-DAB ligand produces yet another intermediate (**4″**) irrespective of the solvent used. From the three unknown species **3‴**, **3*(S)** and **4″**, the structure of **3*(S)** can most easily be established by comparison with that of a stable analogue. For, the ν(CO) IR pattern of **3*(S)** (2085 m,

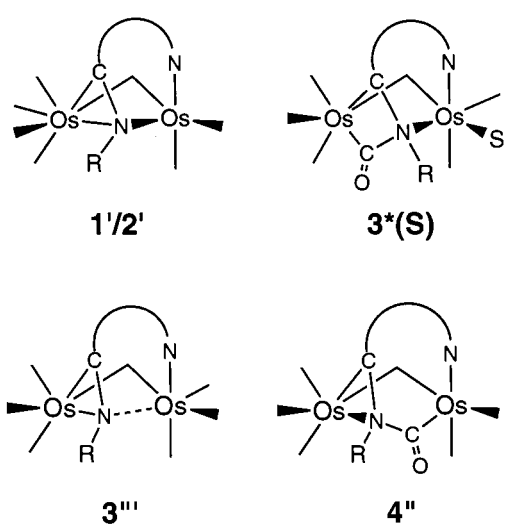

Fig. 5. Proposed structures for the intermediates **1′/2′**, **3*(S)**, **3‴** and **4″**. The bridging $Os(CO)_4$ groups have been omitted for clarity.

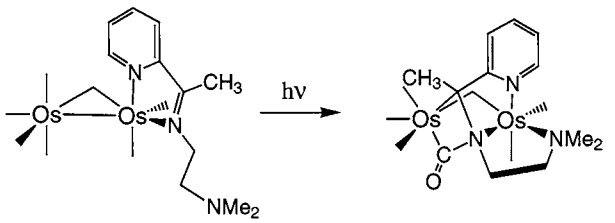

Fig. 6. Photoconversion of $Os_3(CO)_{10}(Me_2N–(CH_2)_2–AcPy)$ (**5**) into its Os–C(O)–N–Os bridged photoproduct (**5***). The bridging $Os(CO)_4$ groups have been omitted for clarity.

2037 s, 2004 vs, 1990 s, 1970 m, 1951 m, 1932 w, 1692 vw cm^{-1}, see Table 2), formed out of the intermediate zwitterion **3b**, is virtually identical to that of the stable cluster **5*** (ν(CO): 2085 m, 2038 vs, 2007 s, 1999 vs, 1990 s, 1970 w, 1955 m, 1924 m, 1703w cm^{-1}). Cluster **5***, the structure of which has been determined by X-ray diffraction [35], is obtained by irradiation of $Os_3(CO)_{10}(Me_2N–(CH_2)_2–AcPy)$ (**5**), in which $Me_2N–(CH_2)_2–AcPy$ is a potentially terdentate R-AcPy ligand bonded as a chelate to one Os atom. The photoconversion of **5** into **5*** is schematically depicted in Fig. 6. According to the structure of **5***, the imine group of the $Me_2N–(CH_2)_2–AcPy$ ligand bridges between two Os centres, just as in the case of **1a**–**4a**. However, contrary to the latter isomeric products of **1-4**, a CO ligand has not yet moved from one Os centre to the other. It has inserted into an osmium–nitrogen bond, which is also evident from the presence of a weak ν(CO) band at 1703 cm^{-1} in the IR spectrum. As in the case of **1a**–**4a**, the η^2-bonding of the imine (and the CO insertion) makes the $Os(CO)_2(Me_2N–(CH_2)_2–AcPy)$ moiety of **5*** coordinatively unsaturated. To compensate for this effect, the pendant Me_2N-group of the terdentate ligand becomes weakly coordinated to the osmium atom of that moiety. As intermediate **3*(S)** has the same ν(CO) band pattern, it must have a very similar structure, in which the pendant Me_2N-group is replaced by a solvent (butyronitrile) molecule (see Fig. 5). Coordination of the solvent plays a crucial role since **3*(S)** is only formed in a coordinating solvent such as butyronitrile via the zwitterion **3b**. The different donor properties of butyronitrile and the $Me_2N–(CH_2)_2$ sidearm are reflected in a lower frequency of the bridging-CO vibration of **3*(S)** (1692 cm^{-1}) compared to that of **5*** (1703 cm^{-1}).

Irradiation of **3** at low temperature in a non-coordinating solvent produces **3‴** as an intermediate instead of **3*(S)**. It has no MLCT band in the visible region, no bridging carbonyl ligand and its CO-stretching frequencies closely correspond to those of the isomeric product **3a**. Apparently, the carbonyl ligand, still on its way from one Os atom to the other in **3*(S)** (and also in **4″**, vide infra), has already moved to the $Os(CO)_2$(α-diimine) moiety in **3‴**, although the final structure of **3a** has not yet been reached. Most probably, the structure of **3‴** merely differs from that of **3a** in the coordination of its imine nitrogen atom; in **3‴** this nitrogen atom may either bind to a single Os centre or form an asymmetric bridge between the two Os atoms (Fig. 5). In the final product **3a** the nitrogen atom forms an Os–N–Os bridge with virtually equal Os–nitrogen bond lengths (Fig. 3) [31].

Contrary to **3**, cluster **4** produces only a single observable intermediate **4″** at low temperature, irrespective of the coordinating ability of the solvent. The structure of **4″** will therefore differ from that of **3‴** and **3*(S)**, and this is confirmed by the IR spectra. Although intermediate **4″** possesses a very low ν(CO) frequency (1721 cm^{-1} in 2-chlorobutane, 1708 cm^{-1} in butyronitrile) just as **3*(S)**, the overall ν(CO) patterns of these two intermediates are very different (Fig. 4c). In the case of **3*(S)** a solvent molecule binds to the $Os(CO)_2$(^{i}Pr-DAB) fragment while a CO ligand bridges between the imine nitrogen atom and the other Os atom. The low ν(CO) frequency points to the presence of a similar N–CO–Os bridge in both **3*(S)** and **4″**. However, the latter intermediate lacks the stabilising effect of a solvent molecule as in the case of **3*(S)**. It is therefore proposed that this stabilisation, i.e. the lifting of the coordinative unsaturation of the Os-α-diimine fragment, is reached in the case of **4″** by the formation of a CO-bridge between the imine nitrogen and the Os atom of the $Os(CO)_2$(neoPent-DAB) moiety (Fig. 5). Going from **4″** to **4‴** (the hypothetical analogue of **3‴**) and **4a**, the CO ligand then reaches its final destination by transforming the $Os(CO)_2$(neoPent-DAB) into an $Os(CO)_3$(neoPent-DAB) moiety.

3.5. The reaction mechanism

Based on the structures of the intermediates, a reaction mechanism is presented for the photoisomerization of **1**–**4** (Scheme 2). We restrict ourselves to the reaction in non-coordinating solvents, where most intermediates could be observed. The first step after excitation is homolysis of a metal–metal bond. This reaction leads to the formation of a biradical species. The biradical undergoes an intramolecular coupling reaction between the two radical sites, leading to the regeneration of the parent cluster as the major product, and to the formation of a small amount of the isomeric species **1a**–**4a**. The quantum yield of the latter reaction is low and strongly influenced by steric effects (Table 3). For instance, the reaction is not observed for the clusters $Os_3(CO)_{10}$(R-AcPy), in which the α-diimine contains a methyl substituent at its imine carbon atom. Species **1′**/**2′**are the first intermediates of this reaction. The imine bond is already η^2-coordinated to the neighbouring metal atom, but the CO groups are still unaffected. The next step is proposed to be the first step in the

CO-shift reaction, viz. insertion of a CO group of the $Os(CO)_4$ fragment into the Os–N bond. In apolar solvents this intermediate **3*** is most probably too short-lived to be observed. It could, however, be stabilized and characterized as **3*(S)** by performing the reaction in the coordinating solvent butyronitrile. Such a stabilization by a coordinating solvent is understandable as it prevents the next step in the reaction, viz. CO insertion into the other Os–N bond (**4″**). Finally, a CO ligand moves to a terminal position at the diimine coordinated Os center, which becomes an $Os(CO)_3$(α-diimine) moiety (**3‴**). This is evident from the close correspondence between the IR ν(CO) pattern of this intermediate and those of the final isomeric products **1a**–**4a**. It is proposed that the transformation of **4″** to **4a** (and the same holds for the other clusters) proceeds in two steps: first a transformation of the CO-bridged **4″** into intermediate **4‴** (the hypothetical analogue of **3‴**) with only a minor change in the imine coordination, then a rearrangement of the imine group to give a final product with two virtually equal Os–N distances (**4a**).

This mechanism is very revealing, since it shows along which route the CO ligands of a cluster may move to overcome a mismatch between the coordination of two metal atoms. This does of course not imply that the CO-shift is the action of a single, specific, CO ligand. All CO ligands of a cluster are known to exchange rapidly and the route depicted in Scheme 2 merely presents a few intermediate stations of a much more complicated dynamic process.

4. Conclusion

The intermediates detected at low temperature allow us to propose an interesting mechanism for the photoisomerization of $Os_3(CO)_{10}$(α-diimine) clusters. The mechanism is of course tentative since structural information on the unstable intermediates can only be scarce and their involvement in the same sequence of events is not completely certain.

Acknowledgements

We thank Professor Dr A. Oskam for fruitful discussions and H. Luyten for his continued technical support.

References

[1] D.J. Stufkens, in: I. Bernal (Ed.), Stereochemistry of Organometallic and Inorganic Compounds, Elsevier, Amsterdam, 1989, p. 226.
[2] A.E. Stiegman, D.R. Tyler, Coord. Chem. Rev. 63 (1985) 217.
[3] T.J. Meyer, J.V. Caspar, Chem. Rev. 85 (1985) 187.
[4] G.L. Geoffroy, M.S. Wrighton, Organometallic Photochemistry, Academic Press, New York, 1979.
[5] A.F. Hepp, M.S. Wrighton, J. Am. Chem. Soc. 105 (1983) 5934.
[6] I.R. Dunkin, P. Harter, C.J. Shields, J. Am. Chem. Soc. 106 (1984) 7248.
[7] T. van der Graaf, D.J. Stufkens, A. Oskam, K. Goubitz, Inorg. Chem. 30 (1991) 599.
[8] M.W. Kokkes, D.J. Stufkens, A. Oskam, Inorg. Chem. 24 (1985) 4411.
[9] D.J. Stufkens, Comments Inorg. Chem. 13 (1992) 359.
[10] D.L. Morse, M.S. Wrighton, J. Am. Chem. Soc. 98 (1976) 3931.
[11] J.C. Luong, R.A. Faltynek, M.S. Wrighton, J. Am. Chem. Soc. 102 (1980) 7892.
[12] J.C. Luong, R.A. Faltynek, M.S. Wrighton, J. Am. Chem. Soc. 101 (1979) 1597.
[13] D.J. Stufkens, Coord. Chem. Rev. 104 (1990) 39.
[14] M.W. Kokkes, W.G.J. de Lange, D.J. Stufkens, A. Oskam, J. Organomet. Chem. 294 (1985) 59.
[15] M.W. Kokkes, D.J. Stufkens, A. Oskam, Inorg. Chem. 24 (1985) 2934.
[16] R.R. Andréa, W.G.J. de Lange, D.J. Stufkens, A. Oskam, Inorg. Chem. 28 (1989) 318.
[17] H.K. van Dijk, D.J. Stufkens, A. Oskam, Inorg. Chem. 28 (1989) 75.
[18] H.K. van Dijk, J. van der Haar, D.J. Stufkens, A. Oskam, Inorg. Chem. 28 (1989) 75.
[19] P.C. Servaas, G.J. Stor, D.J. Stufkens, A. Oskam, Inorg. Chim. Acta 178 (1990) 185.
[20] T. van der Graaf, A. van Rooy, D.J. Stufkens, A. Oskam, Inorg. Chim. Acta 187 (1991) 133.
[21] J.W.M. van Outersterp, D.J. Stufkens, A. Vlček Jr, Inorg. Chem. 34 (1995) 5183.
[22] B.D. Rossenaar, E. Lindsay, D.J. Stufkens, A. Vlček Jr, Inorg. Chim. Acta 250 (1996) 5.
[23] H.A. Nieuwenhuis, A. van Loon, M.A. Moraal, D.J. Stufkens, A. Oskam, K. Goubitz, J. Organomet. Chem. 492 (1995) 165.
[24] M.P. Aarnts, D.J. Stufkens, M.P. Wilms, E.J. Baerends, A. Vlček Jr., I.P. Clark, M.W. George, J.J. Turner, Chem. Eur. J. 2 (1996) 1556.
[25] M.P. Aarnts, D.J. Stufkens, A. Vlček Jr, Inorg. Chim. Acta 266 (1997) 37.
[26] T. van der Graaf, R.M.J. Hofstra, P.G.M. Schilder, M. Rijkhoff, D.J. Stufkens, J.G.M. van der Linden, Organometallics 10 (1991) 3668.
[27] J.W.M. van Outersterp, M.T. Garriga Oostenbrink, H.A. Nieuwenhuis, D.J. Stufkens, F. Hartl, Inorg. Chem. 34 (1995) 6312.
[28] J. Nijhoff, M.J. Bakker, F. Hartl, D.J. Stufkens, W.-F. Fu, R. van Eldik, Inorg. Chem. 37 (1998) 661.
[29] E. Hunstock, F. Hartl, M.J. Calhorda (manuscript in preparation).
[30] R. Zoet, G. van Koten, K. Vrieze, A.J.M. Duisenberg, A.L. Spek, Inorg. Chim. Act. 148 (1988) 71.
[31] R. Zoet, J.T.B.H. Jastrzebski, G. van Koten, T. Mahabiersing, K. Vrieze, D. Heÿdenrÿk, C.H. Stam, Organometallics 7 (1988) 2108.
[32] C.J. Kleverlaan, F. Hartl, D.J. Stufkens, J. Photochem. Photobiol. A: Chem. 103 (1997) 231.
[33] J. Nijhoff, PhD Thesis, Universiteit van Amsterdam, 1998.
[34] J. Víchová, F. Hartl, A. Vlček Jr, J. Am. Chem. Soc. 114 (1992) 10903.
[35] J. Nijhoff, F. Hartl, D.J. Stufkens, J. Fraanje (manuscript in preparation).
[36] H.G. Heller, J.R. Langan, J. Chem. Soc. Perkin Trans. II (1981) 341.
[37] S.o.C.a.A.C. Aberchromics Ltd., College of Cardiff, University of Wales.